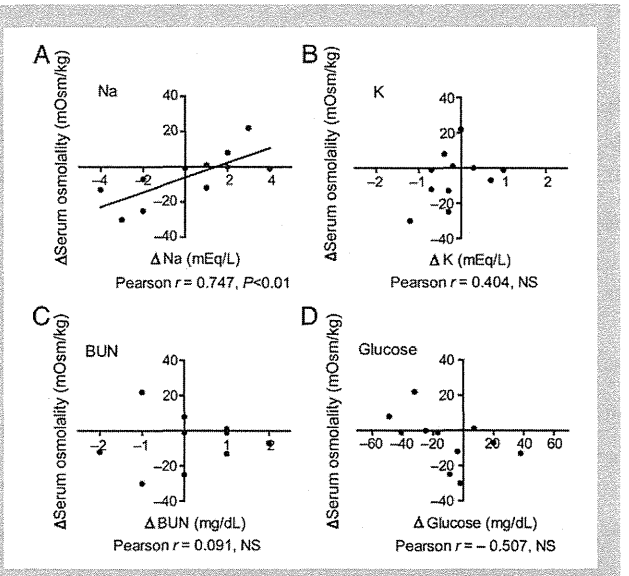

Figure 7 Relation between the degree of change in serum osmolality and that in osmolyte levels. (*A*) Degree of change in serum osmolality was correlated with that in Na^+ concentration in preterm infants ($n = 11$). *X*- and *Y*-axes indicate the degree of change in serum Na^+ concentration and that in serum osmolality, respectively, between Day 0 and Day 1–2. *r*: correlation coefficient. (*B*–*D*) Relation between the degree of change in serum osmolality and the degree of change in levels of three osmolytes in the same infants. *X*-axes in *B*, *C*, and *D* indicate the degree of changes in K^+, BUN, and glucose, respectively, and *Y*-axes indicate the degree of change in serum osmolality between Day 0 and Day 1–2. NS: not significant.

they tend to give fluid supplementation in smaller quantities. Furthermore, water evaporation and loss are greater among extremely preterm infants because of their immature and thin skin.[45] Concentrating urine is also insufficient, due to hypo-responsiveness to arginine vasopressin.[46] These factors may all contribute to increased serum osmolality among extremely preterm infants,[47] and thus might worsen PDA, as implied by our study. Thus, it seems reasonable to propose that keeping their serum osmolality at the proper, but not high, level may be important among preterm infants at risk for PDA.

In conclusion, serum osmolality is transiently decreased after birth, and this decrease may be a physiological mechanism to facilitate DA contraction. It may be time to reconsider the importance of serum osmolality in postnatal adaptation, especially among extremely preterm infants, who are most likely to develop PDA. Maintaining proper serum osmolality may be a clinically meaningful approach to improve the therapeutic outcome of such patients with PDA.

Supplementary material

Supplementary material is available at *Cardiovascular Research* online.

Acknowledgements

The authors are grateful to Yuka Sawada and Naoki Nicho for technical assistance.

Conflict of interest: none declared.

Funding

This work was supported by grants from The Japan Society for the Promotion of Science (grant nos: 22591205 to R.A.; 25293236, 24659100, and 23116514 to U.Y.; 25860614 to Y.Ic.; 23390277 to S.M.; 24390200, 25670131, and 22136009 to Y.Is.), and Shusanki-Iryoukankyou-Seibijigyou (support programmes to improve the Perinatal Care Environment Through Personnel Development) (R.A.), as well as by grants from the Ministry of Health, Labor and Welfare (Y.Is.), the Yokohama Foundation for Advanced Medical Science (U.Y., Y.Ic., and S.M.), the Takeda Science Foundation (U.Y., S.M., and Y.Is.), and a grant for the Research and Development Project of Yokohama City University (Y.Is.).

References

1. Noori S, Stavroudis T, Seri I. Principles of developmental cardiovascular physiology and pathophysiology. In: Kleinman CS, Seri I, eds. *Hemodynamics and Cardiology: Neonatology Questions and Controversies*. 2nd edn. Philadelphia: Elsevier Saunders; 2012. p. 3–27.
2. Koch J, Hensley G, Roy L, Brown S, Ramaciotti C, Rosenfeld CR. Prevalence of spontaneous closure of the ductus arteriosus in neonates at a birth weight of 1000 grams or less. *Pediatrics* 2006;**117**:1113–1121.
3. Nemerofsky SL, Parravicini E, Bateman D, Kleinman C, Polin RA, Lorenz JM. The ductus arteriosus rarely requires treatment in infants > 1000 grams. *Am J Perinatol* 2008;**25**: 661–666.
4. Hamrick SE, Hansmann G. Patent ductus arteriosus of the preterm infant. *Pediatrics* 2010; **125**:1020–1030.
5. Noori S, McCoy M, Friedlich P, Bright B, Gottipati V, Seri I, Sekar K. Failure of ductus arteriosus closure is associated with increased mortality in preterm infants. *Pediatrics* 2009;**123**:e138–e144.
6. Mirea L, Sankaran K, Seshia M, Ohlsson A, Allen AC, Aziz K, Lee SK, Shah PS. Treatment of patent ductus arteriosus and neonatal mortality/morbidities: adjustment for treatment selection bias. *J Pediatr* 2012;**161**:689–694.e1.
7. Clyman RI, Couto J, Murphy GM. Patent ductus arteriosus: are current neonatal treatment options better or worse than no treatment at all? *Semin Perinatol* 2012;**36**: 123–129.
8. Malviya MN, Ohlsson A, Shah SS. Surgical versus medical treatment with cyclooxygenase inhibitors for symptomatic patent ductus arteriosus in preterm infants. *Cochrane Database Syst Rev* 2013;**3**:CD003951.
9. Reeve HL, Tolarova S, Nelson DP, Archer S, Weir EK. Redox control of oxygen sensing in the rabbit ductus arteriosus. *J Physiol* 2001;**533**:253–261.
10. Michelakis E, Rebeyka I, Bateson J, Olley P, Puttagunta L, Archer S. Voltage-gated potassium channels in human ductus arteriosus. *Lancet* 2000;**356**:134–137.
11. Nakanishi T, Gu H, Hagiwara N, Momma K. Mechanisms of oxygen-induced contraction of ductus arteriosus isolated from the fetal rabbit. *Circ Res* 1993;**72**:1218–1228.
12. Yokoyama U, Minamisawa S, Adachi-Akahane S, Akaike T, Naguro I, Funakoshi K, Iwamoto M, Nakagome M, Uemura N, Hori H, Yokota S, Ishikawa Y. Multiple transcripts of Ca^{2+} channel alpha1-subunits and a novel spliced variant of the alpha1C-subunit in rat ductus arteriosus. *Am J Physiol Heart Circ Physiol* 2006;**290**:H1660–H1670.
13. Akaike T, Jin MH, Yokoyama U, Izumi-Nakaseko H, Jiao Q, Iwasaki S, Iwamoto M, Nishimaki S, Sato M, Yokota S, Kamiya Y, Adachi-Akahane S, Ishikawa Y, Minamisawa S. T-type Ca^{2+} channels promote oxygenation-induced closure of the rat ductus arteriosus not only by vasoconstriction but also by neointima formation. *J Biol Chem* 2009;**284**:24025–24034.
14. Smith GC. The pharmacology of the ductus arteriosus. *Pharmacol Rev* 1998;**50**:35–58.
15. Yokoyama U, Minamisawa S, Ishikawa Y. Regulation of vascular tone and remodeling of the ductus arteriosus. *J Smooth Muscle Res* 2010;**46**:77–87.
16. Yokoyama U, Iwatsubo K, Umemura M, Fujita T, Ishikawa Y. The prostanoid EP4 receptor and its signaling pathway. *Pharmacol Rev* 2013;**65**:1010–1052.
17. Jain L, Chen XJ, Ramosevac S, Brown LA, Eaton DC. Expression of highly selective sodium channels in alveolar type II cells is determined by culture conditions. *Am J Physiol Lung Cell Mol Physiol* 2001;**280**:L646–L658.
18. Bland RD. Loss of liquid from the lung lumen in labor: more than a simple 'squeeze'. *Am J Physiol Lung Cell Mol Physiol* 2001;**280**:L602–L605.
19. Modi N. Clinical implications of postnatal alterations in body water distribution. *Semin Neonatol* 2003;**8**:301–306.
20. Feldman W, Drummond KN. Serum and urine osmolality in normal full-term infants. *Can Med Assoc J* 1969;**101**:73–74.
21. Bourque CW, Oliet SH. Osmoreceptors in the central nervous system. *Annu Rev Physiol* 1997;**59**:601–619.
22. Liedtke W, Friedman JM. Abnormal osmotic regulation in $trpv4^{-/-}$ mice. *Proc Natl Acad Sci USA* 2003;**100**:13698–13703.
23. Grimm C, Kraft R, Sauerbruch S, Schultz G, Harteneck C. Molecular and functional characterization of the melastatin-related cation channel TRPM3. *J Biol Chem* 2003;**278**: 21493–21501.
24. Oberwinkler J, Phillipp SE. TRPM3. *Handbook Exp Pharmacol* 2007;**179**:253–267.

25. Yokoyama U, Minamisawa S, Quan H, Ghatak S, Akaike T, Segi-Nishida E, Iwasaki S, Iwamoto M, Misra S, Tamura K, Hori H, Yokota S, Toole BP, Sugimoto Y, Ishikawa Y. Chronic activation of the prostaglandin receptor EP4 promotes hyaluronan-mediated neointimal formation in the ductus arteriosus. *J Clin Invest* 2006;**116**:3026–3034.
26. Yokoyama U, Minamisawa S, Katayama A, Tang T, Suzuki S, Iwatsubo K, Iwasaki S, Kurotani R, Okumura S, Sato M, Yokota S, Hammond HK, Ishikawa Y. Differential regulation of vascular tone and remodeling via stimulation of type 2 and type 6 adenylyl cyclases in the ductus arteriosus. *Circ Res* 2010;**106**:1882–1892.
27. Straub I, Krugel U, Mohr F, Teichert J, Rizun O, Konrad M, Oberwinkler J, Schaefer M. Flavanones that selectively inhibit TRPM3 attenuate thermal nociception in vivo. *Mol Pharmacol* 2013;**84**:736–750.
28. Straub I, Mohr F, Stab J, Konrad M, Philipp SE, Oberwinkler J, Schaefer M. Citrus fruit and fabacea secondary metabolites potently and selectively block TRPM3. *Br J Pharmacol* 2013;**168**:1835–1850.
29. Hong Z, Hong F, Olschewski A, Cabrera JA, Varghese A, Nelson DP, Weir EK. Role of store-operated calcium channels and calcium sensitization in normoxic contraction of the ductus arteriosus. *Circulation* 2006;**114**:1372–1379.
30. Wagner TF, Loch S, Lambert S, Straub I, Mannebach S, Mathar I, Dufer M, Lis A, Flockerzi V, Philipp SE, Oberwinkler J. Transient receptor potential M3 channels are ionotropic steroid receptors in pancreatic beta cells. *Nat Cell Biol* 2008;**10**:1421–1430.
31. Lee N, Chen J, Sun L, Wu S, Gray KR, Rich A, Huang M, Lin JH, Feder JN, Janovitz EB, Levesque PC, Blanar MA. Expression and characterization of human transient receptor potential melastatin 3 (hTRPM3). *J Biol Chem* 2003;**278**:20890–20897.
32. Naylor J, Li J, Milligan CJ, Zeng F, Sukumar P, Hou B, Sedo A, Yuldasheva N, Majeed Y, Beri D, Jiang S, Seymour VA, McKeown L, Kumar B, Harteneck C, O'Regan D, Wheatcroft SB, Kearney MT, Jones C, Porter KE, Beech DJ. Pregnenolone sulphate- and cholesterol-regulated TRPM3 channels coupled to vascular smooth muscle secretion and contraction. *Circ Res* 2010;**106**:1507–1515.
33. Wagner TF, Drews A, Loch S, Mohr F, Philipp SE, Lambert S, Oberwinkler J. TRPM3 channels provide a regulated influx pathway for zinc in pancreatic beta cells. *Pflugers Arch* 2010; **460**:755–765.
34. Majeed Y, Tumova S, Green BL, Seymour VA, Woods DM, Agarwal AK, Naylor J, Jiang S, Picton HM, Porter KE, O'Regan DJ, Muraki K, Fishwick CW, Beech DJ. Pregnenolone sulphate-independent inhibition of TRPM3 channels by progesterone. *Cell Calcium* 2012;**51**:1–11.
35. Vriens J, Owsianik G, Hofmann T, Philipp SE, Stab J, Chen X, Benoit M, Xue F, Janssens A, Kerselaers S, Oberwinkler J, Vennekens R, Gudermann T, Nilius B, Voets T. TRPM3 is a nociceptor channel involved in the detection of noxious heat. *Neuron* 2011;**70**:482–494.
36. Hughes S, Pothecary CA, Jagannath A, Foster RG, Hankins MW, Peirson SN. Profound defects in pupillary responses to light in TRPM-channel null mice: a role for TRPM channels in non-image-forming photoreception. *Eur J Neurosci* 2012;**35**:34–43.
37. Ishizaka H, Kuo L. Endothelial ATP-sensitive potassium channels mediate coronary microvascular dilation to hyperosmolarity. *Am J Physiol* 1997;**273**:H104–H112.
38. Massett MP, Koller A, Kaley G. Hyperosmolality dilates rat skeletal muscle arterioles: role of endothelial K(ATP) channels and daily exercise. *J Appl Physiol* 2000; **89**:2227–2234.
39. Klose C, Straub I, Riehle M, Ranta F, Krautwurst D, Ullrich S, Meyerhof W, Harteneck C. Fenamates as TRP channel blockers: mefenamic acid selectively blocks TRPM3. *Br J Pharmacol* 2011;**162**:1757–1769.
40. Trotter A, Maier L, Pohlandt F. Management of the extremely preterm infant: is the replacement of estradiol and progesterone beneficial? *Pediatr Drugs* 2001;**3**:629–637.
41. Zelenina M, Zelenin S, Aperia A. Water channels (aquaporins) and their role for postnatal adaptation. *Pediatr Res* 2005;**57**:47R–53R.
42. Song Y, Ma T, Matthay MA, Verkman AS. Role of aquaporin-4 in airspace-to-capillary water permeability in intact mouse lung measured by a novel gravimetric method. *J Gen Physiol* 2000;**115**:17–27.
43. Stephens BE, Gargus RA, Walden RV, Mance M, Nye J, McKinley L, Tucker R, Vohr BR. Fluid regimens in the first week of life may increase risk of patent ductus arteriosus in extremely low birth weight infants. *J Perinatol* 2008;**28**:123–128.
44. Bell EF, Acarregui MJ. Restricted versus liberal water intake for preventing morbidity and mortality in preterm infants. *Cochrane Database Syst Rev* 2008;**1**:CD000503.
45. Hammarlund K, Sedin G, Stromberg B. Transepidermal water loss in newborn infants. VIII. Relation to gestational age and post-natal age in appropriate and small for gestational age infants. *Acta Paediatr Scand* 1983;**72**:721–728.
46. Bonilla-Felix M. Development of water transport in the collecting duct. *Am J Physiol Renal Physiol* 2004;**287**:F1093–F1101.
47. Baumgart S, Langman CB, Sosulski R, Fox WW, Polin RA. Fluid, electrolyte, and glucose maintenance in the very low birth weight infant. *Clin Pediatr (Phila)* 1982;**21**:199–206.

J Physiol 592.24 (2014) pp 5461–5475

The Journal of Physiology

Role of cyclic AMP sensor Epac1 in masseter muscle hypertrophy and myosin heavy chain transition induced by β_2-adrenoceptor stimulation

Yoshiki Ohnuki[1], Daisuke Umeki[1,2], Yasumasa Mototani[1], Huiling Jin[3], Wenqian Cai[3], Kouichi Shiozawa[1], Kenji Suita[3], Yasutake Saeki[1], Takayuki Fujita[3], Yoshihiro Ishikawa[3] and Satoshi Okumura[1,3]

[1]*Department of Physiology, Tsurumi University School of Dental Medicine, Yokohama 230-8501, Japan*
[2]*Department of Orthodontics, Tsurumi University School of Dental Medicine, Yokohama 230-8501, Japan*
[3]*Cardiovascular Research Institute, Yokohama City University Graduate School of Medicine, Yokohama 236-0004, Japan*

Key points

- Epac (exchange protein directly activated by cyclic AMP (cAMP)), a PKA-independent cAMP sensor, plays important roles in multiple cellular processes, but its role in the pathogenesis of skeletal muscle hypertrophy and myosin heavy chain (MHC) transition is poorly understood.
- Chronic stimulation of β_2-adrenoceptor (β_2-AR) with clenbuterol (CB), a selective β_2-AR agonist, induced masseter muscle hypertrophy in wild-type (WT) mice, but not in Epac1-null mice (Epac1KO), even if slow-to-fast MHC isoform transition was similarly induced by CB treatment in both WT and Epac1KO.
- Disruption of Epac1 inhibited development of masseter muscle hypertrophy concomitantly with decreased phosphorylation of Akt and its downstream molecules 70 kDa ribosomal S6 kinase 1 and eukaryotic initiation factor 4E-binding protein 1, and also, in parallel, glycogen synthase kinase-3β.
- Disruption of Epac1 decreased histone deacetylase 4 (HDAC4) phosphorylation on serine 246 mediated by calmodulin kinase II (CaMKII), which plays a role in skeletal muscle hypertrophy.
- We conclude that Epac1 induces β_2-AR-mediated masseter muscle hypertrophy without influencing slow-to-fast MHC isoform transition, probably via activation of Akt and its downstream molecules and increase of CaMKII-mediated HDAC4 phosphorylation.

Abstract The predominant isoform of β-adrenoceptor (β-AR) in skeletal muscle is β_2-AR and that in the cardiac muscle is β_1-AR. We have reported that Epac1 (exchange protein directly activated by cAMP 1), a new protein kinase A-independent cAMP sensor, does not affect cardiac hypertrophy in response to pressure overload or chronic isoproterenol (isoprenaline) infusion. However, the role of Epac1 in skeletal muscle hypertrophy remains poorly understood. We thus examined the effect of disruption of Epac1, the major Epac isoform in skeletal muscle, on masseter muscle hypertrophy induced by chronic β_2-AR stimulation with clenbuterol (CB) in Epac1-null mice (Epac1KO). The masseter muscle weight/tibial length ratio was similar in wild-type (WT) and Epac1KO at baseline and was significantly increased in WT after CB infusion, but this increase was suppressed in Epac1KO. CB treatment significantly increased the proportion of myosin heavy chain (MHC) IIb at the expense of that of MHC IId/x in both WT and Epac1KO, indicating that Epac1 did not mediate the CB-induced MHC isoform transition towards the faster isoform. The mechanism of suppression of CB-mediated hypertrophy in Epac1KO is considered to involve decreased activation of Akt signalling. In addition, CB-induced histone deacetylase 4 (HDAC4) phosphorylation on serine 246 mediated by calmodulin kinase II (CaMKII), which plays a role in skeletal muscle hypertrophy, was suppressed in Epac1KO. Our findings suggest that Epac1 plays a role in β_2-AR-mediated masseter muscle hypertrophy, probably through activation of both Akt signalling and CaMKII/HDAC4 signalling.

DOI: 10.1113/jphysiol.2014.282996

(Received 25 August 2014; accepted after revision 8 October 2014; first published online 24 October 2014)
Corresponding author S. Okumura: Department of Physiology, Tsurumi University School of Dental Medicine, 2-1-3 Tsurumi, Tsurumi-ku, Yokohama 230-8501, Japan. Email: okumura-s@tsurumi-u.ac.jp

Abbreviations AR, adrenergic receptor; cAMP, cyclic adenosine 3′,5′-cyclic monophosphate; CaMKII, calmodulin kinase II; CB, clenbuterol; CREB, cAMP response element binding protein; CSA, cross-sectional area; 4E-BP1, eukaryotic initiation factor 4E-binding protein 1; Epac, exchange protein activated by cAMP; Epac1KO, Epac1-deficient mice; ERK1/2, extracellular signalling regulated kinase 1/2; GSK-3β, glycogen synthase kinase-3β; HDAC4, histone deacetylase 4; HE, haematoxylin and eosin; I.P., intraperitoneal injection; mATPase, myofibrillar actomyosin ATPase; MEF2, myocyte enhancer factor 2; MHC, myosin heavy chain; mTOR, mammalian target of rapamycin; NADH-TR, NADH-tetrazodium reductase; NFAT, nuclear factor of activated T cells; NS, not significant; PI3K, phosphoinositol 3-kinase; PKA, protein kinase A; S6K1, 70 kDa ribosomal S6 kinase 1; WT, wild-type.

Introduction

For many decades, it was believed that the major target of cyclic AMP (cAMP) signaling is protein kinase A (PKA). Recently, exchange protein directly activated by cAMP (Epac) was identified as a new PKA-independent sensor. Epac has two isoforms (Epac1 and Epac2). Epac1 is ubiquitously expressed, including in skeletal muscle, and has a single cAMP-binding site, whereas Epac2 contains a second cAMP-binding site and is localized to brain and endocrine tissue (de Rooij *et al.* 1998; Kawasaki *et al.* 1998). We have recently demonstrated that Epac1 does not affect the development of cardiac hypertrophy in response to pressure-overload or chronic isoproterenol infusion, using Epac1-deficient mice (Epac1KO) (Okumura *et al.* 2014). However, the role of Epac1 in skeletal muscle hypertrophy remains poorly understood.

Although all three β-adrenergic receptor (β_1-, β_2-, and β_3-AR) are expressed in the cytoplasmic membrane of skeletal muscle, β_2-subtype is predominant, while β_1-AR accounts for less than 10%, together with small populations of α-AR and β_3-AR (Kim *et al.* 1991). In contrast to skeletal muscle, the predominant receptor subtype expressed in heart is β_1-AR, together with approximately 20% β_2-AR (Woo and Xiao, 2012). All adrenoceptors belong to the guanine nucleotide-binding G protein-coupled receptor family. The G protein-adenylyl cyclase-cAMP is the best characterized of the β_2-AR signaling pathways and is generally thought to be responsible for β_2-AR-mediated hypertrophy and increase of muscle strength with slow-to-fast myosin heavy chain (MHC) isoform transition in skeletal muscle (Ohnuki *et al.* 2013*a*). The hypertrophic response of skeletal muscle following treatment with a chronic β_2-agonist such as clenbuterol (CB) is associated with an increase of protein synthesis, a decrease of protein degradation, or a combination of both mechanisms (Lynch and Ryall, 2008).

Unlike β_1-AR, which couples only to Gsα, β_2-AR also couples to pertussis toxin-sensitive Giα protein in skeletal muscle (Gosmanov *et al.* 2002). β_2-AR-Giα signaling not only inhibits PKA activity, but also stimulates the G$\beta\gamma$-mediated phosphoinositol 3-kinase (PI3K)-Akt and extracellular signaling regulated kinase 1/2 (ERK1/2) signaling pathway (Zhu *et al.* 2001; Shi *et al.* 2007). It was recently reported by us that Akt phosphorylation and subsequent activation of mammalian target of rapamycin (mTOR) are involved in masseter muscle hypertrophy and ERK1/2 phosphorylation exerts an opposing effects on mechanical-overload-induced masseter muscle hypertrophy (Umeki *et al.* 2013). It was recently reported that β-AR signaling activated Epac1 signaling in rat skeletal muscle and β-AR-induced Epac1 activation potentiated insulin-stimulated Akt phosphorylation on serine 473, as well as phosphorylation of its downstream factors 70-kDa ribosomal S6 kinase 1 (S6K1) on threonine 389 (Brennesvik *et al.* 2005). However, the role of Epac1 in skeletal muscle hypertrophy has not been examined yet. We thus hypothesized that Epac1, a major skeletal muscle isoform, might play a role in masseter muscle hypertrophy and MHC isoform transition by linking cAMP signaling and Akt signaling or ERK signaling, and we tested this hypothesis using Epac1KO (Okumura *et al.* 2014).

Methods

Mice and experimental protocols

We have previously reported the generation of Epac1KO (ACC. No. CDB0542K: http://www.cdb.riken.jp/arg/mutant%20mice%20list.htm) (Suzuki *et al.* 2010). All experiments were performed on C57BL/6 and CBA mixed-background homozygous Epac1KO (6.8 $\pm$ 0.3-month-old, n = 12) and their wild-type (WT) littermates (6.4 $\pm$ 0.4-month-old, n = 12). This study was approved by the Animal Care and Use Committees of Yokohama City University School of Medicine and Tsurumi University.

CB (Sigma, St. Louis, MO, USA) was dissolved in saline to prepare a 0.6 mg ml^{-1} stock solution and the appropriate volume of this solution to provide the desired dose (2 mg kg^{-1}) was added to 0.2 ml of saline to prepare the solution for intraperitoneal (I.P.) injection (Pearen *et al.* 2009; Goodman *et al.* 2011). CB was administered I.P. once daily for 3 weeks, and control mice received an identical volume of saline only (Wong *et al.* 1998).

(Fig. 1*A*). In order to minimize the adverse effects associated with repeated I.P. administrations such as infection, inflammation, pain, and adhesions within the abdominal cavity, we followed the recommended protocols for the intraperitoneal injection of mice (Turner *et al.* 2011a, 2011b; Machholz *et al.* 2012). Briefly, we used the recommended gauge and length of needle (22 gauge, 1 inch), scrubbed the injection site gently with 2% chlorhexidine-moistened cotton wool, prepared CB with the recommended volume of saline (maximum 10 ml kg^{-1}), and changed the site of injection every time. In addition, body weight, food and water intake were monitored for all animals throughout the 3 weeks of the experimental period.

The dose of CB used in this study has been reported to increase skeletal mass efficiently without affecting body weight (Ryall *et al.* 2002). After the completion of each treatment, mice were anaesthetized with isoflurane and the left and right masseter muscles were each excised and weighed, frozen in liquid nitrogen, and stored at −80°C for later analysis. The muscle mass (mg) and the ratio of muscle mass to tibial length (mm) were used as indexes of muscle growth. After tissue extraction, the mice were killed by cervical dislocation (Goodman *et al.* 2011).

Western blotting

The right masseter muscle excised from the mice (Fig. 1*A*) was homogenized in a Polytron (Kinematica AG, Lucerne, Switzerland) in ice-cold RIPA buffer (Thermo Fisher Scientific, Waltham, MA, USA: 25 mM Tris-HCl (pH 7.6), 150 mM NaCl, 1% NP-40, 1% sodium deoxycholate, 0.1% SDS) without addition of inhibitors (Yu *et al.* 2011), and

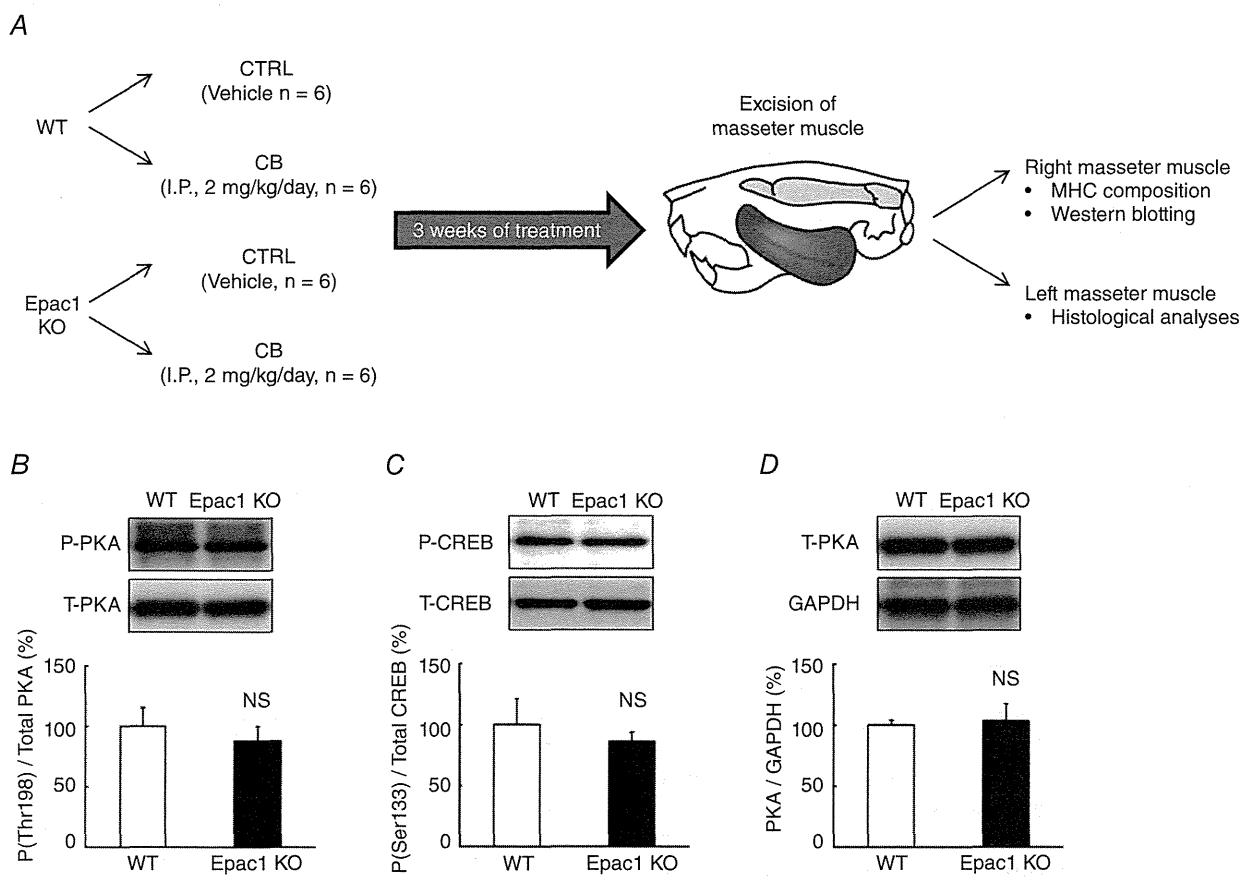

Figure 1. Experimental procedure and cAMP/PKA signaling in Epac1KO
A, clenbuterol (CB) was administered once daily for 3 weeks via intraperitoneal injection (I.P.) at a dose of 2 mg/kg, dissolved in saline. Age-matched control mice (CTRL) received an identical volume of saline only. *B-D*, cAMP/PKA signaling in masseter muscle of Epac1KO was investigated by examining the expression of PKA-catalytic units phosphorylated at threonine (Thr) 198 (*B*), cAMP response element binding protein (CREB) phosphorylated on serine (Ser) 133 (*C*), and total PKA-catalytic units (*D*), using total homogenate prepared from the masseter muscle of Epac1KO and WT. No significant difference was observed between WT and Epac1KO at baseline ($n = 6$ each, P = NS (not significant) *vs.* WT by unpaired t test). The amount of expression in WT treated with saline was taken as 100% in each determination and representative immunoblotting results are shown for phosphorylated and total PKA-catalytic unit, phosphorylated and total CREB, and PKA-catalytic units and GAPDH.

the homogenate was centrifuged at 13000 x *g* for 10 min at 4°C. The supernatant was collected and the protein concentration was measured using a DC protein assay kit (Bio-Rad, Hercules, CA, USA). Equal amounts of protein (5 μg) were subjected to 12.5% SDS-polyacrylamide gel electrophoresis and blotted onto 0.2 mm PVDF membrane (Millipore, Billerica, MA, USA).

Western blotting was conducted with commercially available antibodies (Okumura *et al.* 2003a; Okumura *et al.* 2003b; Okumura *et al.* 2008; Okumura *et al.* 2009; Bai *et al.* 2012). The primary antibodies against CREB (#9197), phospho-CREB (Ser-133, #9198), Akt (#9272), phospho-Akt (Ser-473, #9271), S6K1 (#9202), phospho-S6K1 (Thr-389, #9205), 4E-BP1 (#9644), phospho-4E-BP1 (Thr-37/46, #2855), GSK-3β (#12456) phospho-GSK-3β (Ser-19, #5558), CaMKII (#3362), phospho-CaMKII (Thr-286, #3361), HDAC4 (#7628), phospho-HDAC4 (Ser-246, #3443), ERK1/2 (#4695), phospho-ERK1/2 (Thr-202/Tyr-204, #4370) were purchased from Cell Signaling Technology (Boston, MA, USA) and the primary antibodies against PKA-catalytic subunit (sc-903), phospho-PKA-catalytic subunit (Thr-198, sc-32968), GAPDH (sc-25778), NFATc1 (sc-13033), phospho-NFATc1 (Ser-259, sc-32979), NFATc3 (sc-8321), phospho-NFATc3 (Ser-265, sc-32982) were purchased from Santa Cruz Biotechnology (Santa Cruz, CA, USA) (Lunde *et al.* 2011). Horseradish peroxidase-conjugated anti-rabbit IgG (GB Healthcare, NA934) was used as a secondary antibody. The primary and secondary antibodies were diluted in Tris-buffered saline (pH 7.6) with 0.1% Tween 20 and 5% bovine serum albumin. The blots were visualized with enhanced chemiluminescence solution (ECL Prime Western Blotting Detection Reagent, GE Healthcare, Piscataway, NJ, USA) and scanned with a densitometer (LAS-1000, Fuji Photo Film, Tokyo, Japan).

Diameter and cross-sectional area of muscle fibres

The left masseter muscle, excised as a whole (Fig. 1*A*), was embedded in Tissue-Tek OCT compound (Sakura Finetec, Torrance, CA, USA) in a slightly stretched state so as to maintain a length close to the resting length (L0), and stored it at -80°C until sectioning, as reported (Bruusgaard *et al.* 2012). Cross sections (10 μm thick) were cut from the middle portion of the left masseter muscle with a cryostat (CM1900, Leica Microsystems, Nussloch, Germany) at −20°C. The section were air-dried and fixed with 4% paraformaldehyde in 0.1 M phosphate-buffered saline (pH 7.5). The sections were then stained with hematoxylin and eosin (HE) and observed under a light microscope (BX61, Olympus Co., Tokyo, Japan). Micrographs were taken with a digital camera (DP-72, Olympus Co.) connected to a personal computer. The cross-sectional size of muscle fibres was evaluated by measuring the minimal diameter of muscle fibres (in order to correct for obliquely cut muscle fibres) and the cross-sectional area (CSA) (Kiliaridis *et al.* 1988; Okumura *et al.* 2003*b*). The minimal diameter and CSA of 100 muscle fibres in the superficial portion were measured with image analysis software (Image J 1.45) and averaged to obtain the mean values in each mouse.

MHC composition

MHC isoform composition in masseter muscle was analysed by means of SDS-PAGE, followed by silver staining of the bands of each MHC isoform (Silver Staining Kit, GE Healthcare, Uppsala, Sweden). The stained bands were scanned with a densitometer (LAS-1000, Fuji Photo Film, Tokyo, Japan). To determine the MHC composition, the relative proportion of each MHC isoform was calculated as a percentage of total MHC content using the integrated dye density of the bands (Ohnuki *et al.* 1999; Ohnuki and Saeki, 2008; Ohnuki *et al.* 2009; Ohnuki *et al.* 2013b).

Histochemistry

Myofibrillar actomyosin ATPase (mATPase) staining with pre-incubation at pH 4.6 or pH 10.6, as well as NADH-tetrazodium reductase (NADH-TR) staining, was performed as described previously (Hamalainen and Pette, 1993; Sartorius *et al.* 1998). mATPase staining with pre-incubation at pH 4.6 enables distinction of type IIA fibre (light) and type IID/X (dark) or type IIB fibres (dark) and mATPase staining with pre-incubation at pH 10.6 enables distinction of type IIB fibres (light) and type IIA (dark) or type IID/X fibres (dark). NADH-TR staining visualizes the oxidative capacity of muscle fibres.

Statistical analysis

Data are expressed as means ± SEM. The statistical significance of difference was determined using student's unpaired *t* test (Fig. 1*B–D*) or a two-way ANOVA (genotype and treatment main effects, and interaction effect) where appropriate (Figs 2*A–C*, *E–F*, 3*B*, 4*B*, 5, and 6). Tukey's *post hoc* test was used to examine simple treatment main effects and to identify significant differences between Control and CB-treated groups in WT or Epac1KO (Figs 2*A–C*, *E–F*, 3*B*, 4*B*, 5, and 6). The criterion of significance was taken as $P < 0.05$.

Results

PKA signalling was not altered in Epac1KO

We first examined whether or not cAMP/PKA signalling in masseter muscle of Epac1KO was altered by examining the expression of PKA signalling proteins in total homogenates

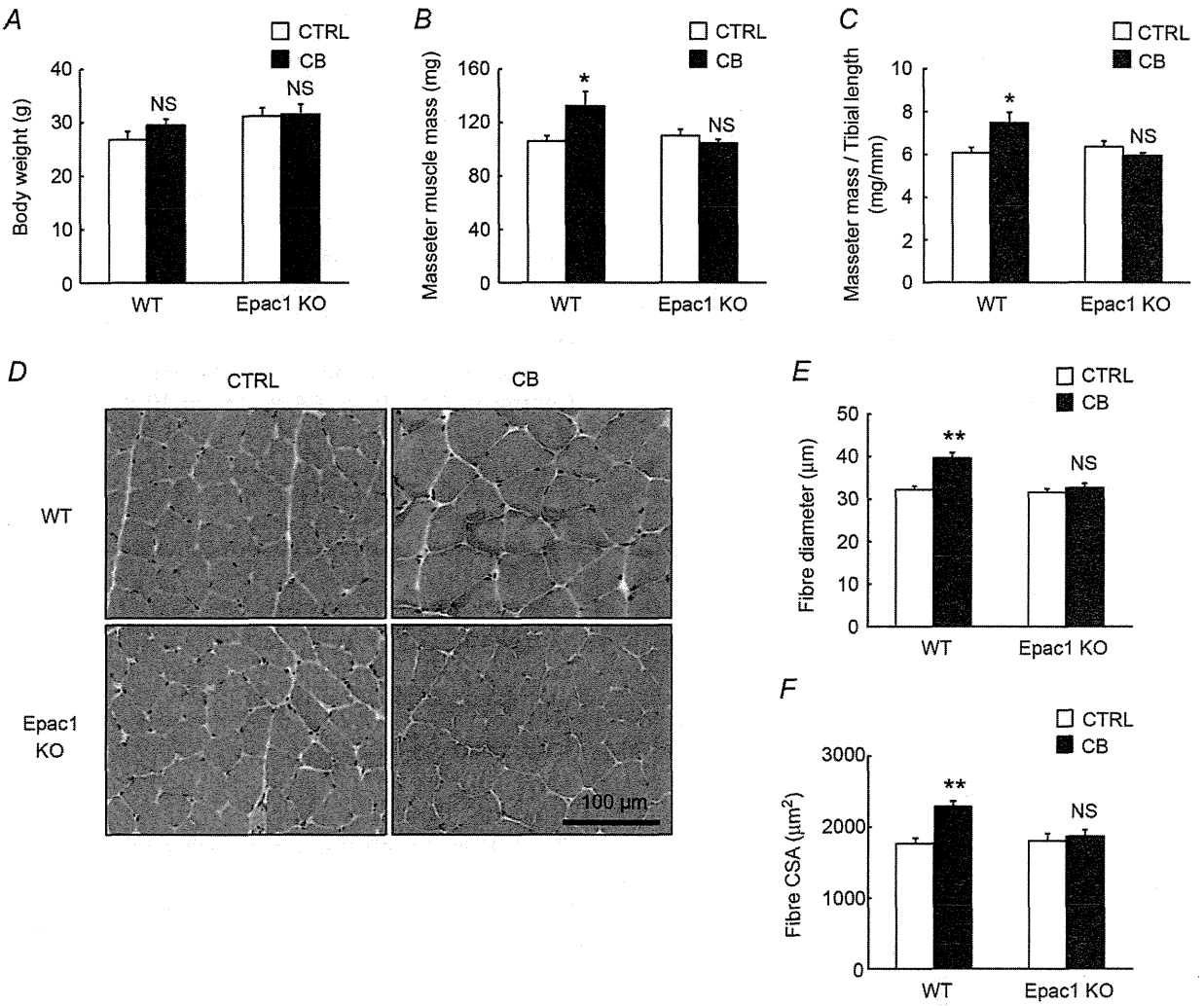

Figure 2. Effects of CB on body weight, masseter mass and histological analysis
Body weight (*A*), masseter muscle mass (*B*), masseter muscle mass to tibial length ratio (*C*), cross sections of masseter muscle (*D*), fibre diameter(*E*) and fibre cross-sectional area (CSA) (*F*) of masseter muscle prepared from CB-treated (CB) and age-matched control (CTRL) WT and Epac1KO. *A*, no significant difference in body weight was observed between the control (CTRL) and CB-treated group in either WT (CTRL *vs.* CB: 27 ± 1.6 *vs.* 29 ± 1.2 g, P = NS by Tukey's *post hoc* test, $n = 6$) or Epac1KO (CTRL *vs.* CB: 31 ± 1.5 *vs.* 32 ± 1.9 g, P = NS by Tukey's *post hoc* test, $n = 6$). *B* and *C*, both the masseter muscle mass and the masseter muscle mass to tibial length ratio were significantly increased by the CB treatment in WT (masseter muscle mass: CTRL *vs.* CB: 106 ± 4.4 *vs.* 133 ± 10.5 mg; masseter muscle mass/tibial length (mg/mm): CTRL *vs.* CB: 6.1 ± 0.2 *vs.* 7.5 ± 0.5, $^*P < 0.05$ by Tukey's *post hoc* test, $n = 6$), but these increases were suppressed in Epac1KO (masseter muscle: CTRL *vs.* CB: 110 ± 4.9 *vs.* 104 ± 2.4 mg; masseter muscle mass/tibial length (mg/mm): CTRL *vs.* CB: 6.4 ± 0.3 *vs.* 5.9 ± 0.1, P = NS by Tukey's *post hoc* test, $n = 6$). *D–F*, typical cross-sections of HE staining (*D*), fibre diameter (*E*), and fibre cross sectional area (CSA) (*F*) of masseter muscle in control and CB-treated WT and Epac1KO. Fibre diameter was significantly increased by CB treatment in WT (from 32 ± 0.8 to 40 ± 1.3 mm, $^{**}P < 0.01$ by Tukey's *post hoc* test, $n = 6$), but no increase was observed in Epac1KO (from 32 ± 0.8 to 33 ± 1.0 mm, P = NS by Tukey's *post hoc* test, $n = 6$) (*E*). Fibre CSA was also similar in WT and Epac1KO at baseline (WT *vs.* Epac1KO: 1762 ± 80 *vs.* 1800 ± 107 μm^2, P = NS by Tukey's *post hoc* test, $n = 6$) (*F*). It was significantly increased by CB treatment in WT (from 1762 ± 80 to 2284 ± 80 μm^2, $^{**}P < 0.01$ by Tukey's *post hoc* test, $n = 6$), while this increase was suppressed in Epac1KO (from 1800 ± 107 to 1866 ± 92 μm^2, P = NS by Tukey's *post hoc* test, $n = 6$).

prepared from masseter muscles of Epac1KO and WT controls (Altarejos and Montminy, 2011). PKA-catalytic units phosphorylated at threonine 198 (WT *vs.* Epac1KO: 100 ± 15 *vs.* 88 ± 12%, P = NS (not significant) by unpaired t test, n = 6 each) (Fig. 1*B*), cAMP response element binding protein (CREB) phosphorylated on serine 133 (WT *vs.* Epac1KO: 100 ± 21 *vs.* 86 ± 7%, P = NS by unpaired t test, n = 6 each) (Fig. 1*C*), and total PKA-catalytic units (WT *vs.* Epac1KO: 100 ± 4 *vs.* 103 ± 15%, P = NS by unpaired t test, n = 6 each) (Fig. 1*D*). Thus, we found no significant difference between Epac1KO and WT control. These data indicated that cAMP/PKA signalling was not altered in the masseter muscle of Epac1KO.

CB-induced masseter muscle hypertrophy was inhibited in Epac1KO

Body weight, masseter muscle mass, and masseter muscle mass to tibial length ratio were examined in 3-week CB-treated and age-matched control WT and Epac1KO mice (Fig. 2). Body weight (Fig. 2*A*, genotype and treatment main effects, and interaction effect, P = NS by two-way ANOVA) was similar in the control and CB-treated groups of WT (Control *vs.* CB: 27 ± 1.6 *vs.* 29 ± 1.2 g, P = NS by Tukey's test, n = 6) as well as Epac1KO (Control *vs.* CB: 31 ± 1.5 *vs.* 32 ± 1.9 g, P = NS by Tukey's test, n = 6). However, the masseter muscle mass (Fig. 2*B*, significant interaction effect, $P < 0.05$ by two-way ANOVA) and the masseter muscle mass to tibial length ratio (Fig. 2*C*, significant interaction effect, $P < 0.05$ by two-way ANOVA) were significantly increased by CB treatment in WT (masseter muscle mass: Control *vs.* CB: 106 ± 4.4 *vs.* 133 ± 10.5 mg; masseter muscle mass/tibial length ratio (mg/mm): Control *vs.* CB: 6.1 ± 0.2 *vs.* 7.5 ± 0.5, P <0.05 by Tukey's test, n = 6). These increases were suppressed in Epac1KO (masseter muscle mass: Control *vs.* CB: 110 ± 4.9 *vs.* 104 ± 2.4 mg; masseter muscle/tibial length ratio (mg/mm): Control *vs.* CB: 6.4 ± 0.3 *vs.* 5.9 ± 0.1, P = NS by Tukey's test, n = 6).

Histological analysis showed no abnormal organization of masseter muscle (such as fibrosis) in either WT or Epac1KO (Fig. 2*D*) and the fibre diameter (Fig. 2*E*, significant interaction effect, $P < 0.01$ by two-way ANOVA) was similar in WT and Epac1KO at baseline (WT *vs.* Epac1KO: 32 ± 0.8 *vs.* 32 ± 0.8 μm, P = NS by Tukey's test, n = 6). However, it was significantly increased by CB treatment in WT (from 32 ± 0.8 to 40 ± 1.3 μm, $P < 0.01$ by Tukey's test, n = 6), while this increase was suppressed in Epac1KO (from 32 ± 0.8 to 33 ± 1.0 μm, P = NS by Tukey's test, n = 6), as was the case for masseter muscle mass.

Fibre CSA (Fig. 2*F*, significant interaction effect, $P < 0.01$ by two-way ANOVA) was also similar in WT and Epac1KO at baseline (WT *vs.* Epac1KO: 1762 ± 80 *vs.* 1800 ± 107 μm^2, P = NS by Tukey's test, n = 6). It was significantly increased by CB treatment in WT (from 1762 ± 80 to 2284 ± 80 μm^2, $P < 0.01$ by Tukey's test, n = 6), while this increase was suppressed in Epac1KO (from 1800 ± 107 to 1866 ± 92 μm^2, P = NS by Tukey's test, n = 6), as was the case for masseter muscle mass as well as fibre diameter.

These data indicate that Epac1 plays an important role in the development of masseter muscle hypertrophy in response to β_2-AR stimulation with CB.

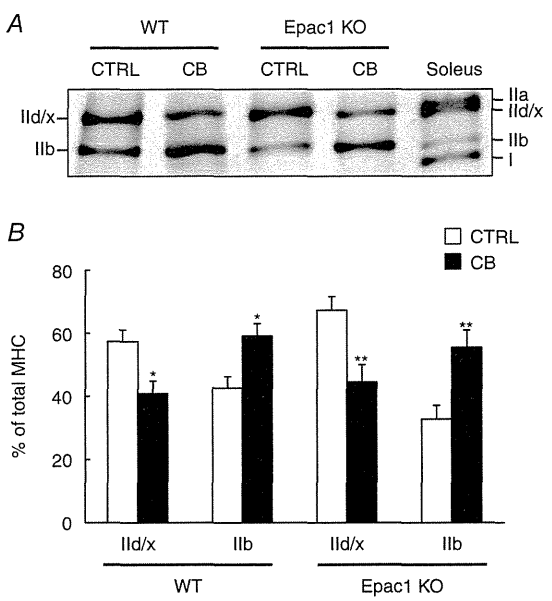

Figure 3. Effects of CB on MHC composition in masseter muscle
Typical SDS-PAGE profiles of MHC isoforms of masseter muscle and soleus muscle (*A*) and the average MHC compositions of masseter muscle (*B*) prepared from CB-treated (CB) and age-matched control (CTRL) in WT and Epac1KO. The relative proportion of each MHC isoform was expressed as a percentage of total MHC content (% of total MHC). In both WT and Epac1KO, the proportion of MHC-IId/x was significantly decreased (WT: from 57 ± 3.7 to 41 ± 4.0%, $^*P < 0.05$ by Tukey's *post hoc* test, n = 6, Epac1KO: from 67 ± 4.4 to 45 ± 5.5%, $^{**}P < 0.01$ by Tukey's *post hoc* test, n = 6), while that of MHC IIb was significantly increased (WT: from 43 ± 3.7 to 59 ± 4.0%, $^*P < 0.05$ by Tukey's *post hoc* test, n = 6, Epac1KO: from 33 ± 4.4 to 55 ± 5.5%, $^{**}P < 0.01$ by Tukey's *post hoc* test, n = 6) after CB treatment (*B*).

CB-induced MHC isoform transition was not altered in Epac1KO

The average MHC isoform compositions in masseter muscle obtained from CB-treated and age-matched control WT and Epac1KO mice were examined by SDS-PAGE analysis (Fig. 3). The masseter muscle is composed primarily of MHC-IId/x and MHC-IIb, which

harness anaerobic metabolism to generate ATP, whereas soleus muscle is composed primarily of MHC-I and MHC-IIa, which utilize oxidative phosphorylation as their energy source, with only a little MHC-IIb (Fig. 3*A*). CB treatment promoted MHC isoform transition towards faster isoforms in both WT and Epac1KO (Fig. 3*B*, significant treatment main effect in MHC-IId/x and MHC-IIb, $P < 0.01$ by two-way ANOVA), i.e. the proportion of MHC-IId/x was significantly decreased (WT: from 57 ± 3.7 to 41 ± 4.0%, $P < 0.05$ by Tukey's

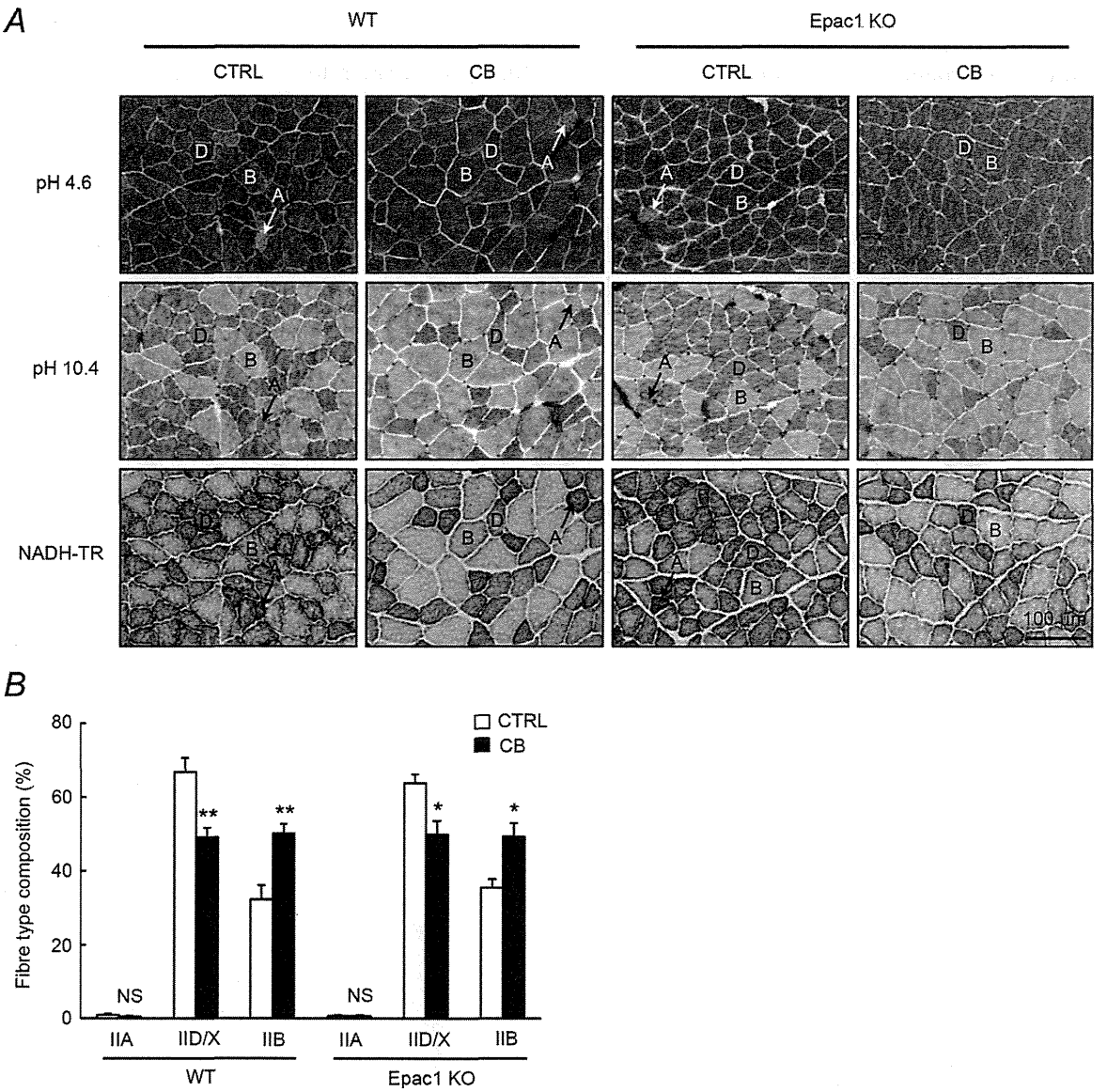

Figure 4. Effects of CB on fibre type composition in masseter muscle
A, typical cross sections of histochemical staining for mATPase with pre-incubation at pH 4.6 (upper), or with pre-incubation at pH 10.4 (middle), and NADH-TR staining (lower) of masseter muscle in control and CB-treated WT (left) and Epac1KO (right). The oxidative capacity of muscle fibres, as presented by NADH-TR staining, showed the following tendency: IIA (dark) > IID/X > IIB (light). Key: A, type IIA; B, type IIB; D, type IID/X. *B*, CB treatment did not alter the proportion of type IIA fibre (IIA) in both WT (from 1.0 ± 0.4 to 0.5 ± 0.2%, P = NS by Tukey's *post hoc* test, $n = 6$) and Epac1KO (from 0.6 ± 0.3 to 0.7 ± 0.3%, P = NS by Tukey's *post hoc* test, $n = 6$). The proportion of type IID/X fibre (IID/X) was significantly decreased in both WT (from 67 ± 3.8 to 49 ± 2.4%, $^{**}P < 0.01$ by Tukey's *post hoc* test, $n = 6$) and Epac1KO (from 64 ± 2.4 to 50 ± 3.6%, $^{*}P < 0.05$ by Tukey's *post hoc* test, n = 6) after the CB treatment. The proportion of type IIB fibre (IIB) was significantly increased in both WT (from 32 ± 3.9 to 50 ± 2.4%, $^{**}P < 0.01$ by Tukey's *post hoc* test, $n = 6$) and Epac1KO (from 36 ± 2.2 to 49 ± 3.7%, $^{*}P < 0.05$ by Tukey's *post hoc* test, $n = 6$) after the CB treatment.

test, $n = 6$; Epac1KO: from 67 ± 4.4 to 45 ± 5.5%, $P < 0.01$ by Tukey's test, $n = 6$), while that of MHC-IIb was significantly increased (WT: from 43 ± 3.7 to 59 ± 4.0%, $P < 0.05$ by Tukey's test, $n = 6$; Epac1KO: from 33 ± 4.4 to 55 ± 5.5%, $P < 0.01$ by Tukey's test, $n = 6$). These data indicated that Epac1 did not influence the slow-to-fast MHC isoform transition in the masseter muscle in response to CB treatment.

In order to confirm the results of SDS-PAGE analysis, we also performed the histochemical staining for mATPase with acid pre-incubation at pH 4.6 (Fig. 4*A*, upper), which enables the distinction of type IIA fibre (containing MHC-IIa) (light) and type IID/X fibre (containing MHC-IId/x) (dark) or type IIB fibre (containing MHC-IIb) (dark), as well as staining for mATPase with alkaline pre-incubation at pH 10.4 (Fig. 4*A*, middle), which enables distinction of type IIB fibre (light) and type IID/X fibre (dark) or type IIA fibre (dark), in addition to NADH-TR staining (Farber *et al.* 1954) (Fig. 4*A*, lower). The proportion of type IIA fibre

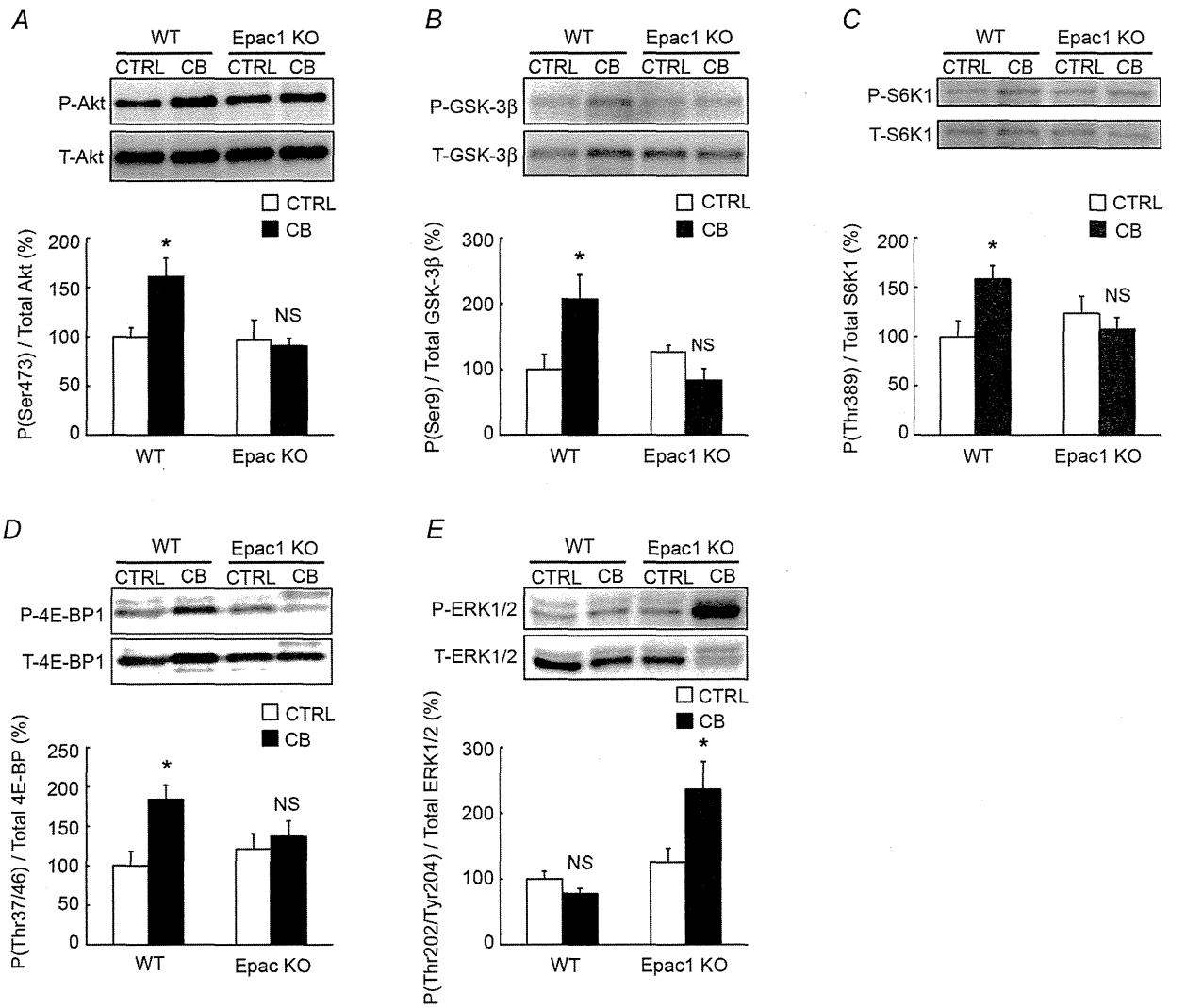

Figure 5. Activities of Akt or ERK1/2 signalling in WT and Epac1KO in response to chronic CB treatment
A–D, the activities of molecules involved in Akt signalling were examined by measuring phosphorylated and total Akt (*A*), GSK-3β (*B*) , S6K1 (*C*), and 4E-BP1 (*D*) in masseter muscle of WT and Epac1KO after chronic CB treatment (2 mg kg^{-1} day^{-1} I.P.) for 3 weeks. Significant activation of these molecules was observed in WT (*$P < 0.05$ by Tukey's *post hoc* test, $n = 5$–6), but not in Epac1KO (P = NS by Tukey's *post hoc* test, $n = 5$–6). *E*, phosphorylation of ERK1/2 was not different between control (CTRL) and CB-treated group in WT (from 100 ± 12 to 79 ± 8%, P = NS by Tukey's *post hoc* test, $n = 5$), but it was significantly increased by approximately two-fold by CB treatment in Epac1KO (from 126 ± 21 to 236 ± 42%, *$P < 0.05$ by Tukey's *post hoc* test, $n = 5$–6). The amount of expression in WT treated with saline was taken as 100% in each determination and representative immunoblotting results are shown for phosphorylated and total Akt, GSK-3β, S6K1, 4E-BP1, EPK1/2.